Subshell photoionization of Xe between 40 and 1000 eV

U. Becker, D. Szostak, H. G. Kerkhoff, M. Kupsch, B. Langer, and R. Wehlitz
Institut für Strahlungs-und Kernphysik, Technische Universität Berlin, Hardenbergstrasse 36, D-1000 Berlin 12, Federal Republic of Germany

A. Yagishita
Photon Factory, National Laboratory for High Energy Physics, Tsukuba, Ibaraki 305, Japan

T. Hayaishi
Institute of Applied Physics, University of Tsukuba, Tsukuba, Ibaraki 305, Japan
(Received 27 September 1988)

Partial cross sections and angular-distribution asymmetry parameters were measured for subshell photoionization of xenon for photon energies between 40 and 1000 eV. These large-scale measurements show that the pronounced interchannel coupling between the valence and the 4*d* electrons persists beyond the 4*d* shape resonance in the subsequent Cooper-minimum region. Multielectron processes associated with 4*d* and 4*p* photoemission were measured directly for the first time over a broader energy range covering the near-threshold behavior up to the sudden limit. Comparing our experimental results with calculations based on the single-particle model shows that this theory, which fails to describe the intermediate energy range even qualitatively for the valence electrons, gives partial cross sections in reasonable agreement with experiment at higher photon energies, particularly beyond the 3*d* threshold. The same result is shown by the angular-distribution asymmetry parameter β, except for the photoionization of the "4*p*" subshell which resembles more the behavior of a 4*d* electron, corroborating the theoretical assumptions of core-hole fluctuations between these two subshells. In the shape resonance region the presented 4*d* partial cross sections are in reasonable agreement with theoretical results obtained recently by many-body perturbation theory.

I. INTRODUCTION

Xenon has become more and more a showcase for atomic inner-shell photoionization.[1–3] Different theoretical models have been used to describe the partial cross sections for subshell photoionization of xenon. For review of the different methods see, for example, Amusia,[4] Starace,[5] and Kelly.[6]

Beyond the generally good qualitative agreement of most theories which take account of electron correlations in one or another way with the experimental data, there arose the question of a more quantitative description of the various partial cross sections, particularly regarding the role and the strengths of multielectron processes in this context.[6] Closely related to this problem is the question of the validity of the single-particle model, in particular Hartree-Fock with complete exchange[7] at higher photon energies where very few experimental data are available because most experiments were concentrated on the intermediate energy range around the 4*d* shape resonance.

Many detailed studies have been performed to determine the partial photoionization cross sections and angular-distribution asymmetry parameters of the Xe subshells. Here we will give a very short survey of the development since the advent of synchrotron radiation as a vacuum ultraviolet (vuv) and soft-x-ray light source for photoionization studies; more references may be found in the following papers. West *et al.*[8] started the series of partial-cross-section measurements using synchrotron radiation with Xe 5*p*, 5*s*, and 4*d*. Besides further studies of this kind the same group also started measurements of angular-distribution asymmetry parameters of the different subshells of xenon (Torop *et al.*[9]). More recent measurements of asymmetry parameters are from Krause *et al.*[10] and Southworth *et al.*,[11] both giving references to other earlier work. Spin-orbit branching ratios were studied by Wuilleumier *et al.*[12] and more recently by Yates *et al.*[13] whereas Fahlmann *et al.*[14] studied multielectron processes associated with the valence photoionization of xenon. All of these measurements concentrated on the intermediate energy from 15 to 150 eV. An extension of these measurements to higher energies was very recently performed by Lindle *et al.*[15] regarding 4*d* subshell photoionization in the Cooper-minim region and "4*p*" photoionization in the same energy region. A first study of partial cross sections and angular-distribution asymmetry parameters of the 3*d* subshell was also very recently performed by Becker *et al.*[16] Most of these papers contain extensive references to other related experimental and theoretical work and give a more or less detailed description of the physical phenomena associated with the photoionization of Xe, in particular the Xe 4*d* subshell; this will not be repeated here.

After Cooper's[17] pioneering work on the Xe 4*d* shape resonance, many theoretical studies were performed re-

garding the Xe photoionization problem. Following the first and still only large-scale study by Kennedy and Manson[7] performed within the single-particle approximation, Amusia and co-workers[18] started to emphasize the importance of many-electron effects in Xe. Various theoretical methods have been employed to treat the many-electron effects, the most recent one being many-body perturbation theory (MBPT).[19]

The purpose of the present work was to complete the presently known data in the intermediate energy range, approaching ultimately curves of partial cross sections instead of a few separated data points; and to extend the experimental data to higher energies beyond the $3d$ threshold up to 1000 eV. Special emphasis was put on three points: interchannel coupling, the direct determination of the strengths of multielectron processes, and the measurement of partial cross sections and angular-distribution asymmetry parameters over a wide energy range. Our data will be compared with former measurements and calculations from different theoretical models. The dynamic range of our measurement covers approximately 4 orders of magnitude in intensity comparing the weakest $5s$ cross section within the Cooper minimum with the most enhanced $4d$ cross section at the shape resonance.

II. EXPERIMENT

The photoemission experiments were performed in part at the electron storage ring BESSY and in part at the Hamburger Synchrotronstrahlungslabor HASYLAB, both under single-bunch conditions. The photoion measurements were performed using the electron storage ring at the Photon Factory. The experiment at BESSY was performed with photons from the high-energy toroidal grating monochromator (HE-TGM 1) between 270 and 1000 eV.[20] The photoemission measurements covering the intermediate energy range from 40 to 170 eV took place at the TGM of HASYLAB.[21] We used the time-of-flight (TOF) method for the partial-cross-section and angular-distribution asymmetry parameter measurements, recording two spectra at different angles by two TOF detectors simultaneously. The measurement of the $4d$ electrons from threshold through the shape resonance is complicated by extended Auger structure resulting from decay of the $4d$ core hole. These NOO Auger electrons cover a wide energy range of about 37 eV (Refs. 22 and 23) and show in addition a continuous distribution due to double Auger processes.[24] In order to take into account all of these electrons, it is necessary to measure the whole photoelectron and Auger spectrum over the entire energy range. Our time-of-flight spectrometer, having a drift length of 650 mm, requires for this purpose a time window of approximately 1 μsec as given by the DORIS storage ring at HASYLAB under single-bunch operation. Figure 1 shows such a spectrum taken at a photon energy of 110 eV. This spectrum shows for the first time clearly the existence of Auger lines with energies as low as 0.5 eV accompanied by an increase of the background near 4 and 2.5 eV most likely due to double Auger decay following the recombination of the $4d_{3/2}$ (N_4) and $4d_{5/2}$ (N_5) core holes.

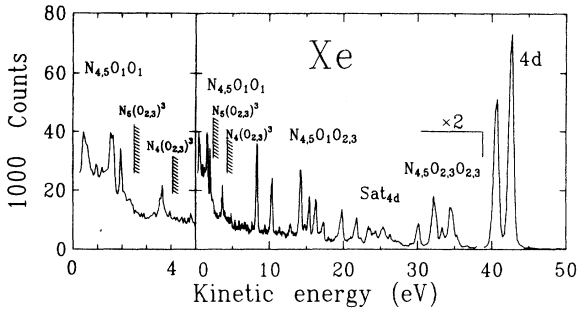

FIG. 1. Photoelectron spectrum of Xe recorded at a photon energy of 110 eV. The spectrum shows in addition to the photolines several previously unobserved NOO Auger transitions below 2 eV, displayed separately on an enlarged scale, and a steplike increase in the background continuum indicating the N_4 and N_5 thresholds of the double Auger decay. The line structure between 22 and 28 eV kinetic energy consits of $4d$ satellites. The spectrum was recorded at an angle of 0° with respect to the photon polarization direction.

One major problem in measuring partial cross sections over an extended energy range is the determination of the intensity of the incoming monochromatized synchrotron radiation. This determination of the actual photon flux depends sensitively on the type of beam monitor used in the photoemission experiment. The different methods commonly in use such as gold-yield measurements,[25] fluorescent efficiency of sodium salicylate,[26] and partial cross sections of the light rare gases He, Ne, and Ar (Ref. 27) vary significantly in accuracy and have both advantages and certain disadvantages. While the first two methods allow one to monitor the photon flux simultaneously with the sampling of the photoelectron spectra, the last one requires a further experiment subsequently or in advance. On the other hand, the partial-cross-section measurements of He, Ne, and Ar determine directly the relevant photon flux in first order at the interaction volume and the corresponding cross sections are relatively well known, in contrast to the yield measurements giving photon flux values integrated over all orders and being taken at a position different from the actual interaction volume. But the most significant disadvantage of the yield method is the efficiency problem, depending on the preparation of the beam monitor, which means that each monitor has to be calibrated separately. More recent studies show[28] that no tabulated values[25] can be used reliably over a broad energy range without consistency checks by other methods. We have therefore used the partial-cross-section method calibrated by simultaneous registration of the beam current in the storage ring in addition to a simultaneously performed gold-yield measurement. This combined method makes it easier to notice possible inconsistencies in the calibration procedure and allows in addition the direct determination of the fraction of higher-order light in the monochromatized photon beam, which is in turn necessary to derive the first-order photon flux from the gold-yield measurement. Details of

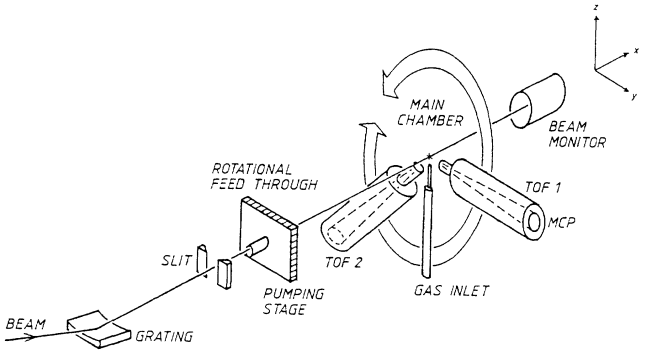

FIG. 2. Schematic representation of an angle-resolved gas-phase photoemission experiment using synchrotron radiation excitation and time-of-flight detection.

the calibration procedure including the determination of the polarization of the monochromatized light and the transmission function of our time-of-flight analyzer system will be given elsewhere.[29] Figure 2 shows a scheme of the experiment using pulsed synchrotron radiation excitation along with angle-resolved time-of-flight electron detection.

The ion-yield measurements performed at the Photon Factory used photons from a 2-m grasshopper monochromator in the energy range between 60 and 180 eV. The spectral resolution was about 0.3 at 100 eV. A Be window was used for the measurements in the range from 60 to 110 eV in order to eliminate the effect of second-order light originating from large yields of the 4*d* partial cross section beyond the delayed onset. The photoions produced by the radiation were charge analyzed by a time-of-flight spectrometer which was operated by a pulsed acceleration field method to eliminate the changing detection efficiencies arising from coincidences with multiple electrons in the electron-ion coincidence method. The ion yields of each charge state were converted into the absolute photoionization cross sections using the total cross sections tabulated by West and Morton.[30] Details of the experimental setup were described in previous publications.[31] Figure 3 shows the results of the ion-yield measurements for Xe^+, Xe^{2+}, and Xe^{3+} in the shape-resonance region. Our ion-yield curves are in good agreement with the former measurements of Holland *et al.*;[32] reasonable agreement with the results of El-Sherbini and Van der Wiel[33] is given only in part for their Xe^{2+} results whereas there is again much better agreement with the improved data of Van der Wiel and Wight for Xe^+.[34] Comparisons to other ion-yield measurements not covering the whole shape-resonance region are given in the above-mentioned references.

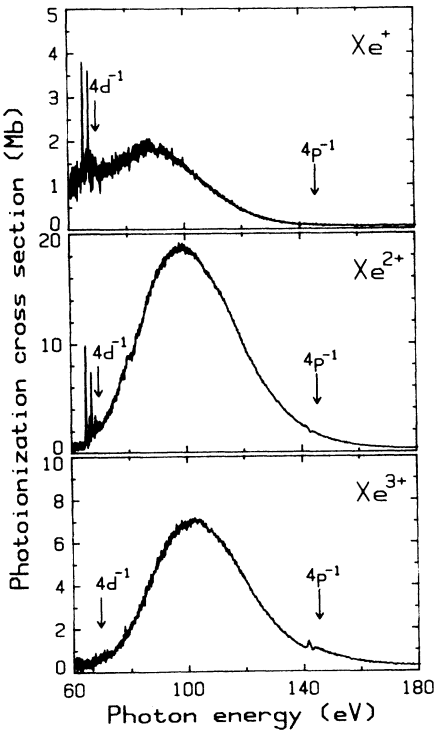

FIG. 3. Ion-yield measurements of Xe^+, Xe^{2+}, and Xe^{3+} taken in the 4*d* shape-resonance region. The arrows show the positions of the 4*d* and 4*p* thresholds, respectively.

III. RESULTS AND DISCUSSION

A. General overview

The combined results of our partial-cross-section measurements are given in Fig. 4. Because of the extended energy range under study and the pronounced intensity variation of the different partial cross sections, part of our results are plotted on a double-logarithmic scale. All of our measurements were brought to an absolute scale by adjusting the sum of all measured photoelectron lines including the multielectron processes to the total cross section at $h\nu = 130$ eV.[30] This particular photon energy was chosen because the corresponding photoelectron spectrum allows most unambiguously the separation of photoelectron from Auger lines, a basic requirement for the correct normalization of the sum of all photolines to the total cross section; furthermore, the results of the different total-cross-section measurements are at this energy in excellent agreement.[30] Our data points are complemented by data from Fahlmann *et al.*[14] for low photon energies and by measurements from Lindle *et al.*[15] in the Cooper-minimum region of the 4*d* partial cross section. The latter were normalized to absolute values by adjusting their 4*d* data points at lowest energies to our corresponding values. These two data sets were chosen for this survey figure because they both cover a large energy range and have sufficient overlap with our own combined data set from the two experiments at HASYLAB and BESSY. The data points from the HE-TGM 1 shown in Fig. 4(b) by solid symbols represent subshell photoionization cross sections including accompanying multielectron processes due to the limited resolution of our spectrometer at higher kinetic energies. The separated 4*d* and 4*p* main line contributions are given by

open symbols for energies below 400 eV. From these data the 4*d* partial cross section at 270 eV was used to calibrate the whole high-energy data set absolutely via the corresponding data points of Lindle *et al.*[15] which were in turn calibrated by our low-energy data set as mentioned above. The Xe 3*d* partial cross section represents the sum of the two main line spin-orbit components. The curves represent calculations within the single-particle model (see Ref. 1). This figure, in particular the comparison with the Hartree-Fock (HF) calculations, shows three noteworthy new features in the behavior of the Xe partial cross sections.

(1) The strong interchannel coupling observed between the 4*d* and 5*p* and 5*s* subshells governing the cross-section behavior of all subshells within the 4*d* shape resonance persists also in the subsequent Cooper-minimum region, an energy range where strong coupling of the 4*d* with the 4*p* subshell was just recently observed.[15] Small effects of interchannel coupling are also seen at the onset of the 3*d* partial cross section.

(2) The single-particle model, which describes the behavior of the 4*d* cross section in the intermediate energy range only qualitatively, gives quantitatively much better results at higher photon energies, especially above the 3*d*

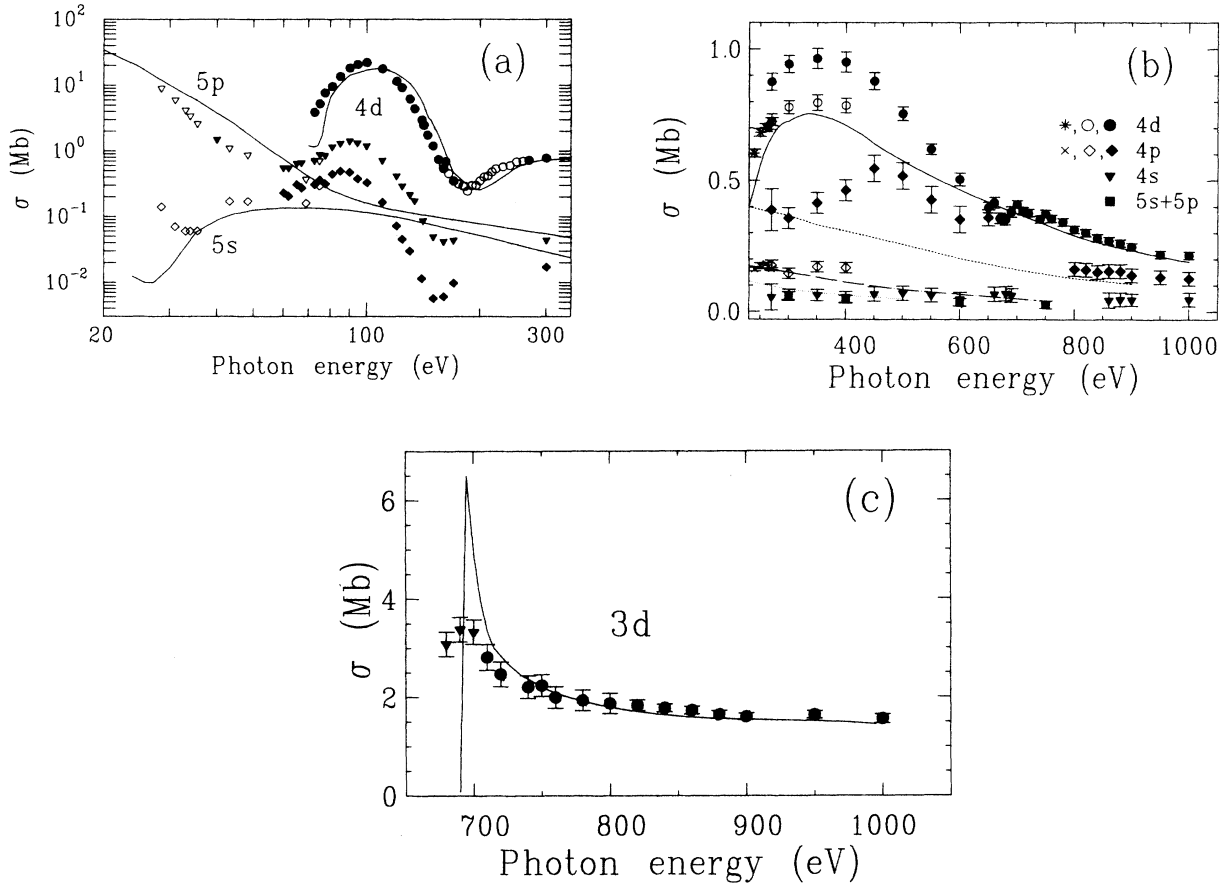

FIG. 4. (a) Partial cross sections of the Xe 5*p* (solid triangles), 5*s* (solid diamonds), and 4*d* (solid circles) subshells between 20 and 300 eV. The reference data of other authors are for 5*p* (open triangles) and 5*s* (open diamonds) from Fahlmann *et al.* (Ref. 14) and for 4*d* (open circles) from Lindle *et al.* (Ref. 15). The absolute normalization of our data and of the values of Ref. 15 is described in the text. The error bars for 5*s* and 5*p* are approximately 10% except for the four smallest 5*s* cross sections having an uncertainty of approximately 25%, and the 4*d* error bars are given explicitly in Fig. 5. The solid curves represent calculations within the independent-particle approximation (HF theory) as given by Krause (Ref. 1). (b) Partial cross sections for Xe 4*d* (circles), 4*p* (diamonds), 4*s* (triangles), and the sum of the 5*s* and 5*p* (squares) subshell photoionization between 270 and 1000 eV. Open symbols for 4*d* and 4*p* represent the intensity of the separated photolines whereas the solid symbols represent the same subshell photoionization cross sections including accompanying multielectron processes. The reference data of Lindle *et al.* (Ref. 15) are given by stars (4*d*) and crosses (4*p*). The data points for the 4*s* subshell represent single-peak intensities, whereas the sum of the 5*s* and 5*p* partial cross sections includes the corresponding satellite intensity. The drawn curves show the same HF calculations as in (a) representing 4*d* by the solid curve, 4*p* by the dashed curve, 4*s* by the dashed-dotted curve, and the sum of 5*s* and 5*p* by the dotted curve. (c) 3*d* subshell photoionization cross section compared with the same HF calculation as in (a) and (b). The solid circles give the sum of the two spin-orbit components without 3*d* satellite intensity. The solid triangles represent the same partial cross section but measured by the corresponding MNN Auger intensity.

threshold for both the 4*d* and 3*d* partial cross section.

(3) At these high photon energies the single-particle model seems to subsume most of the strong multielectron processes known from ionization measurements of the 4*p* and 4*d* subshell at 1487 eV (Al $K\alpha$) (Ref. 35) within the single-electron contributions, because the sum of all photoemission events associated with the ionization of a given subshell is reasonably described by the corresponding Hartree-Fock cross sections. This is in marked contrast to the behavior at intermediate energies.

A quantitative determination of the strengths of some of these multielectron processes will be given later preceding the discussion of the character of the "4*p*" photoline. Regarding the photolines with higher binding energies, the 4*s* line deviates most strongly from the HF calculation. This could be a Cooper minimum in the 4*s* partial cross section shifted to higher energies above threshold by many-electron effects. However, the data analysis of the 4*s* peak area is complicated by "4*p* shake-off" electrons which lie underneath the 4*s* peak, giving rise to serious problems with the correct background determination for this peak. The estimated uncertainties in σ_{4s} resulting from this effect prohibit a more detailed and conclusive comparison with theory. A comparison of our valence results with those of other authors yields good agreement with the data of West *et al.*[8] and Adam *et al.*[36] for the 5*p* and 5*s* partial cross sections within the 4*d* shape-resonance region.

B. 4*d* subshell

Comparing photoionization of the 4*d* subshell with the valence photoionization results shows that there is, regarding the total intensity variation, more serious scatter among the various previous measurements of the 4*d* partial cross section than among the 5*p* and 5*s* data. Table I gives our 4*d* partial cross sections, together with previous 4*d* measurements for data points within an energy interval of 0.5 eV in the shape-resonance region. The variation among the partial-cross-section measurements is most likely caused by the different calibration procedures used in the different experiments. The first measurements of West *et al.*,[8] later improved by Shannon *et al.*,[37] are branching-ratio measurements partitioning the absorption cross section by use of the triple ionization measurements of El-Sherbini and Van der Wiel[33] to correct for multielectron processes. Adam[38] performed an independent determination of the relative change of the 4*d* partial cross section, also using the partition method, but without correcting for 4*d*-based multielectron processes. In contrast to these measurements Becker *et al.*[39] tried to determine the relative change of the partial cross section independently of the partition method by using the gold-yield method to monitor the relative intensity of the photon beam flux quantitatively. Their 4*d* partial cross sections above 95 eV are lower than the other measurements but still in reasonable agreement with the earlier data of

TABLE I. Xe 4*d* partial cross section. The data of this work are compared to the results of earlier measurements within 0.5 eV regarding their energy position. The error bars represent statistical errors and uncertainties in the relative calibration of the photoelectron intensities. The possible systematic error resulting from the absolute calibration is approximately 3% (Ref. 30).

	Partial cross section (4*d*) (Mb)			
Photon energy (eV)	This work	Adam Ref. 38	Shannon *et al.* Ref. 37	Becker *et al.* Ref. 39
72.5	3.9(2)	4.0(8)		4.0(4)
75.0	5.2(3)			7.7(4)
77.5	7.7(4)		7.7(8)	
81.0	9.6(5)	11.4(12)		
85.0	13.6(7)			
90.0	18.3(9)		20(2)	
94.5	20.8(10)		21(2)	21(3)
100.0	22.1(11)			19(3)
110.0	17.8(9)		15.7(16)	12.5(7)
120.0	11.4(6)			6.8(20)
124.0	9.2(5)		7.4(7)	
130.0	6.2(3)			3.6(5)
134.0	4.4(2)		2.2(2)	3.1(5)
140.0	2.98(14)			0.8(5)
141.5	2.49(12)			
142.0	2.46(12)			
145.0	1.74(8)			
150.0	1.19(6)			0.4(4)
155.0	0.74(3)			
160.0	0.75(3)			0.2(3)
162.0	0.69(3)			
170.0	0.35(3)			

West *et al.*[8] within mutual error bars. This seemed to confirm indirectly the assumptions of El-Sherbini and Van der Wiel[33] about the strengths of the shake processes of approximately 20% as a lower limit. Our new measurement, calibrated by the partial-cross-section method using well-known standard cross sections of Ne, shows good agreement with all measurements between 70 and 95 eV but starts to deviate above 100 eV. In this energy range our data points are consistently higher, particularly with respect to the calibration point at 130 eV, than the results obtained by Becker *et al.*[39] by the gold-yield method. This deviation is most likely due to the inherent calibration problems of the latter method as mentioned before. Our values are also partly above the results which West *et al.*[8] obtained by partitioning the total photoionization cross section after correcting for multielectron processes, but below 125 eV much less substantially.

Figure 5(a) shows our partial-cross-section results together with a curve for the total cross section and three

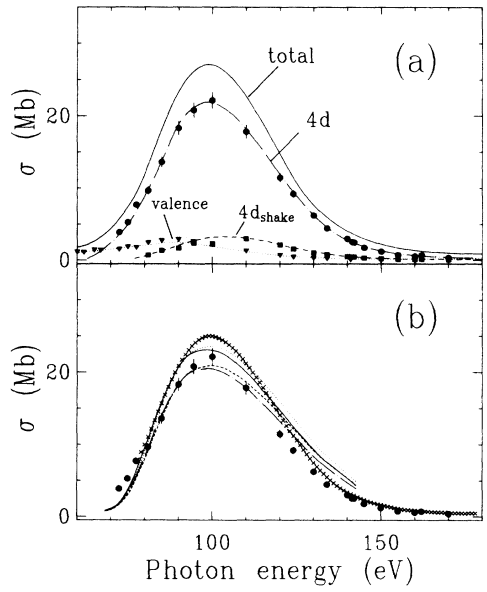

FIG. 5. (a) 4*d* partial cross sections (circles) within the shape resonance along with corresponding data (dash-dotted line) obtained from ion-yield measurements as explained in the text. The triangles represent the valence results of this work $\sigma_v = 1.46$ [1.218 $(\sigma_{5p}+\sigma_{5s})$], while the dotted curve gives the corresponding ion-yield-derived values. The $4d_{\text{shake}}$ (shake-up and shake-off) results derived from direct measurements and from the ion-yield curves are given by the squares and the dashed curve. The solid line represents the total cross section as given by West and Morton (Ref. 30). (b) The same 4*d* partial cross sections, but compared to different theoretical calculations as shown in Ref. 19. The dotted and the solid curves represent MBPT length (L) and velocity (V) calculations with relaxation. The short-dashed curve and the dash-dotted curve represent MBPT calculations with relaxed orbitals, but additionally taking into account overlap integrals between orbitals of the ground state and corresponding orbitals of the final state. The line given by crosses represents the sum of the 4*d* and 4*d* shake curves from (a).

curves derived from our ion-yield measurements as shown in Fig. 3. The data points and their corresponding curves represent (1) the 4*d* partial cross section, (2) all multielectron processes associated with the photoionization of the 4*d* subshell (designated in the following for brevity as "4*d* shake contributions": shake-up and shake-off), and (3) the sum of all partial cross sections related to the photoionization of a valence electron (5*s*, 5*p*). The derivation of these curves is based on the following relations between partial cross sections and ion yields:

$$\sigma_{\text{val}} = 1.46\sigma^{+} ,$$

$$\sigma_{4d} = (1+x)(\sigma^{2+} - 0.46\sigma^{+}) ,$$

$$\sigma_{\text{shake}} = \sigma^{3+} - x(\sigma^{2+} - 0.46\sigma^{+}) ,$$

with x as a normalization constant being related to the fraction of 4*d* hole states decaying via double Auger processes into triply charged ions. The double ionization cross section σ^{2+} is corrected by the valence shake-off contribution which is 46% (Ref. 38) of the 5*p* and 5*s* valence photoionization cross section represented by σ^{+}. We have fitted the ion-yield curves of Xe^{2+} and Xe^{3+} from Fig. 3 according to these relations to our 4*d* partial cross sections and the fractional 4*d* shake intensity as shown in Fig. 6. Note that, for this purpose, the resonances due to double excitations as seen in Fig. 3 were removed from the ion-yield curves because our partial cross sections are basically nonresonant values. One data point on a resonance near 80 eV was omitted for clarity. The solid curves are derived from an x value being approximately 0.21. Regarding the Xe^{3+} ion yield and their relation to the total double Auger rate one should keep in mind that the shake-off transitions yield triply charged ions via direct double ionization followed by normal Auger decay, whereas the shake-up or satellite transitions may yield triple ions through single ionization accompanied by excitation as a first step followed by double Auger decay. More specifically, the relationship between our normalization constant x and the double Auger yield α_{4d} for the main line transitions and α_{sat} for the shake-up or satellite transitions depending on the satellite to main line ratio is given by

$$\frac{1}{1+x} = \alpha_{4d} - (\alpha_{\text{sat}} - 1)\frac{\sigma_{\text{sat}}}{\sigma_{4d}} .$$

A rough estimation of the shake-up or satellite to shake-off ratio yields, above 110 eV, a value of 1.5 for an average of all multielectron processes of 17.5%. If, for example, 50% of the excited ionic 4*d* hole states decay via double Auger transitions, the double Auger rate of the 4*d* hole states associated with the main line would be approximately 22%. A quantitative analysis of the data points below the lowest 4*d* satellite threshold where $\sigma_{\text{sat}}/\sigma_{4d}$ is zero yields an average value of $\alpha_{4d} = 0.215$ and $\alpha_{\text{sat}} = 0.58$, in good accord with this assumption. Further support of this large double Auger yield of excited states (satellite states) is given by recent measurements of the resonant double Auger yield following $4d \rightarrow np$ excitation.[40,41]

The dotted line represents the ion yield derived partial cross section for all valence photoionization processes. The data points are obtained from our 5*p* and 5*s* partial cross sections as shown in Fig. 4 using an average value of 21.8% for the valence shake-up transitions[14] and 46% as shake-off fraction[38] referred to the total-valence single-ionization rate. Hence the total-valence partial cross section σ_v is given by

$$\sigma_v = 1.46|1.218(\sigma_{5p}+\sigma_{5s})| \ .$$

These data points are, near their maximum, somewhat higher than the corresponding curve derived from the cross section for single ionization. However, the consistency and overall agreement of this first combined analysis of partial photoemission cross sections and photoionization yield curves at a shape resonance is very good considering the error bars. In contrast to the behavior of the resonantly enhanced valence photoionization cross section, which has its maximum more than 10 eV below the maximum of the 4*d* shape resonance due to screening effects,[42] the maximum of the 4*d* shake transitions is about 5 eV above this 4*d* maximum. The solid line represents the total cross section as given by West and Morton.[30] The sum of the three contributions shown in this figure, σ_{4d}, $\sigma_{4d\ \mathrm{shake}}$, and σ_{val}, resembles the σ_{tot} curve of West and Morton[30] very closely and is also in good agreement with our total ion yield which was absolutely normalized to σ_{tot}.

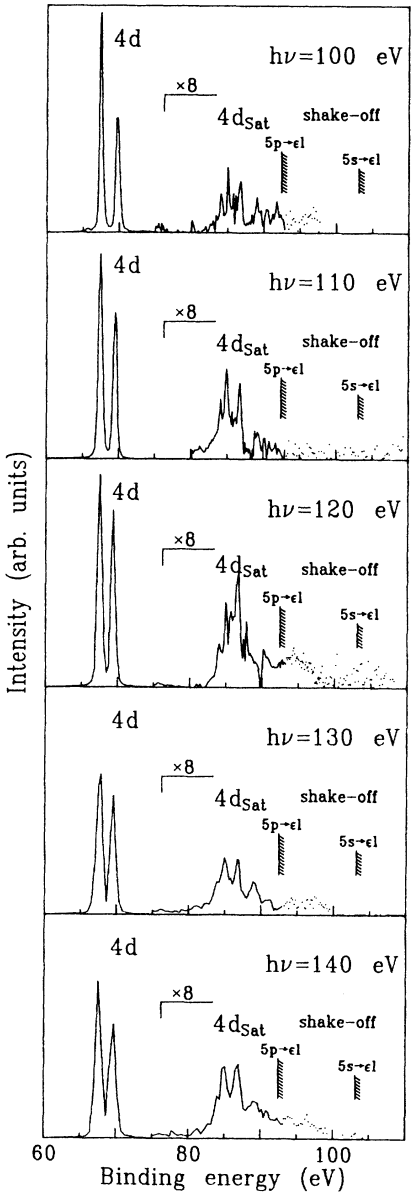

FIG. 6. Photoelectron spectra for $h\nu = 100-140$ eV showing the 4*d* satellite transitions and part of the subsequent shake-off continuum obtained by subtraction of the NOO Auger spectrum.

Figure 5(b) gives a comparison of our 4*d* partial cross sections with the most recent theoretical calculations, by Altun *et al.*[19] The curves represent many-body calculations using relaxed orbitals; the higher pair of curves results from calculations not including an overlap factor and therefore subsuming part of the multielectron processes. Length and velocity calculations are given by the dotted and solid lines, respectively. The lower pair of curves represents again length (dashed) and velocity (dashed-dotted) results: however, this time including the overlap factor which reduces the partial cross section by approximately 11%. These results are in reasonable overall agreement with our 4*d* results. The agreement is very good between 80 and 110 eV; above this energy range the theoretical results are consistently higher than the experimental values, while below this energy range they are too low. The curve given by the crosses is the sum of the 4*d* curve and the 4*d* shake curve in Fig. 5(a) representing all 4*d*-based ionization processes. This curve shows better agreement with the calculations without overlap factor, which one would expect because these calculations should include most of the multielectron processes associated with the 4*d* ionization. The theoretical results are again in excellent agreement for intermediate energies, deviating from the experimental data at lower and higher energies similarly to the 4*d* partial-cross-section results.

Summarizing, one can say that previous inconsistencies between different sets of data could be removed and that there is now satisfactory accord between the different types of experiments including very recent absolute 4*d* partial-cross-section measurements[43] which are in excellent agreement with our data. There is now also reasonable, although not completely satisfactory, agreement between experiment and the most recent calcultions based on MBPT methods, concerning both the 4*d* partial cross section alone and the total 4*d* intensity (which contains in addition most of the associated multielectron processes). Further improvement in the calculations may be obtained by inclusion of higher-order diagrams accounting for double ionization channels.

In order to determine the strengths of the multielectron processes in more detail, we have tried to separate the corresponding shake-electron structure from the 4*d* main line as well as from the Auger transitions. This could be done unambigously only for photon energies just

below the 4*p* excitations (130–140 eV) and at higher photon energies between 300 and 450 eV, due to the limited resolution of our TOF spectrometer for very high kinetic energies and the photon energy gap between the TGM at HASYLAB and the HE-TGM 1 at BESSY. For all other energies the 4*d* Auger structure had to be subtracted in order to reveal the undisturbed satellite structure. Figure 6 displays a series of such spectra for photon energies from 100 to 140 eV. Figure 7 shows in more detail the complex line structure of the multielectron processes associated with the ionization of the 4*d* subshell at different photon energies, including a spectrum of Svensson *et al.*[35] taken with Al $K\alpha$ radiation. The comparison of these three spectra, particularly of the ones at 100 and 1487 eV, suggests the assumption that some of the satellite lines show increasing intensity with increasing photon energy, whereas others seem to be constant or even to decrease relative to others at higher energies, a behavior similar to observations made for valence[44] and *K*-shell photoionization.[45] However, our assumption that different 4*d* satellite lines exhibit different behavior with photon energy has to be proven for individual lines by high-resolution measurements. Figure 8 gives a relative intensity plot of the sum of all multielectron processes covering an energy range from 10 eV above threshold into the regime of the sudden limit, where we have approximately 21% multielectron processes relative to the 4*d* main line. The region between the dotted curves represents the values obtained from the ion-yield measurements as described above. Our results near the maximum of the shape resonance are lower than the assumptions of El-Sherbini and Van der Wiel[33] but approach their value of 20% at higher energies. In the sudden limit, our results are consistent with the total shake-up intensity of 12% reported by Lindle *et al.*,[15] yielding for all multielectron processes (shake-up and shake-off) 20% as a lower limit.

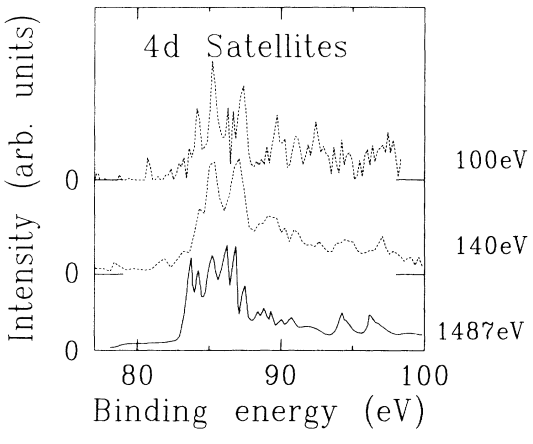

FIG. 7. Enlarged representation of the 4*d* satellite spectra taken at 100 and 140 eV compared to a corresponding spectrum taken at 1487 eV by Svensson *et al.* (Ref. 35).

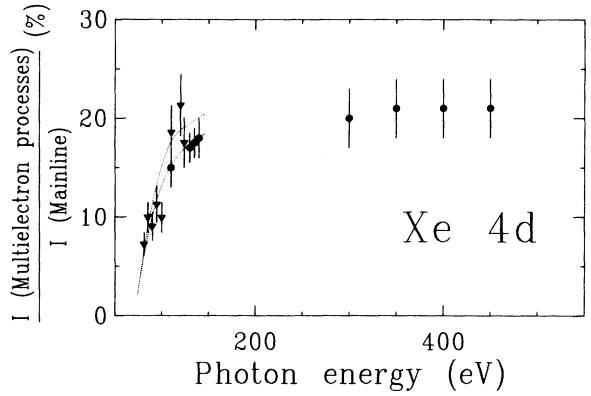

FIG. 8. Branching ratio between the sum of all multielectron processes and the 4*d* main line. The solid circles show the directly measured intensity of the multielectron processes between shake-up energies of 12–22 eV, while the triangles represent the difference between the sum of all partial cross sections and the total cross section. The two sets of data coincide exactly at the normalization point at 130 eV.

C. 4*s* and "4*p*" subshells

The multielectron processes associated with the "4*p*" and 4*s* subshell ionization are significantly stronger than those of the 4*d* subshell. Figure 4(b) shows that they account for approximately 1.5 times the intensity of the "4*p*" main line for photon energies between 300 and 400 eV, a ratio which should be approximately constant also for higher photon energies. The existence of this structured intensity continuum, together with the missing $p_{1/2}$ component of the "4*p*" photoline, gave rise to alternative interpretations of this spectrum in terms of many-body effects, in particular core-hole fluctuations. Wendin and Ohno[46] showed that the dipolar fluctuations of the 4*p* hole prevent the existence of $4p_{1/2}$ and $4p_{3/2}$ hole states as quasistationary states. Instead they find that the most stable and probable state belongs to the configuration $Xe^{+}(4d^{8}4f)_{3/2}$, identifying this state with the main 4*p* photoelectron peak at 145 eV accompanied by $4d^{8}ml$ excitations and a $4d^{8}$ shake-off continuum. If this interpretation regarding the "4*p*" spectrum as strong "4*d*-satellite" and "shake-off" spectrum is true, there should be a stronger similarity between the angular distribution of the "4*p*" photoline and the 4*d* photoline than expected on the basis of the independent-particle model. Figure 9 shows the angular-distribution asymmetry parameter β for the 4*s* and "4*p*" photolines in comparison with the predictions of the HF theory[7] for β_{4p} and an average representation of β_{4d} (Ref. 16) in the same photon energy range. This figure shows that the two sets of experimental β values $\beta_{\text{"}4p\text{"}}$ and β_{4d} coincide very well, in contrast to the poor agreement with the theoretical β_{4p}^{HF} curve. Lindle *et al.*[15] have shown that this similarity extends even into the Cooper-minimum region at lower photon energies. The β values of the 4*s* peak deviate at some few energies from the value $\beta=2$ expected within the single-particle model. This could be the result of many-body

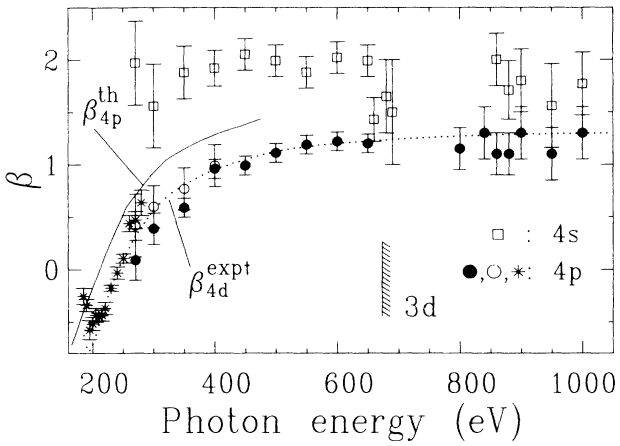

FIG. 9. Angular-distribution asymmetry parameters for the 4*s* (open squares) and "4*p*" (circles) photolines compared to a theoretical curve for the "4*p*" photoline (solid line: HF approximation) and an average curve of the experimental β values of the 4*d* photoline (dotted line: average of β_{4d}^{expt} from Refs. 15 and 16). The open circles represent pure separated "4*p*" contributions, whereas the solid circles represent β values for the sum of the "4*p*" peak and the subsequent "continuum" between "4*p*" and 4*s*. The stars are separated "4*p*" data points from Lindle *et al.* (Ref. 15).

effects on the photoionization of the Xe 4*s* and 4*p* subshells, but also could be caused by the background problems mentioned before. The drop in β seen at the 3*d* threshold may result from interchannel coupling between the 4*s* and 3*d* subshells, an effect observed similarly for the 4*d* angular-distribution asymmetry parameter β_{4d} in the vicinity of the 3*d* threshold recently.[16]

IV. SUMMARY

In conclusion, we have measured partial cross sections and angular-distribution asymmetry parameters β for subshell photoionization of Xe in the vuv and soft-x-ray range. The results for the inner shells are qualitatively described by the single-particle model, in particular for partial cross sections at higher photon energies, in contrast to the outer valence shells which are governed by strong interchannel-coupling effects, especially in the intermediate energy range. The importance of multielectron processes associated with the photoionization of the Xe 4*p* and 4*d* subshells was proven by direct determination of the strengths of these processes in suitable photoelectron spectra, where the different processes could be unambigously separated. In order to evaluate curves of partial cross sections throughout the shape-resonance region, we have performed a combined analysis of photoemission and photoion data. The results for the 4*d* partial cross section within the shape resonance are in generally reasonable agreement with the MBPT calculations, even in part with respect to the separation into single-electron and multielectron processes. The overall comparison with theoretical results shows that the broad-range behavior of the Xe photoionization still awaits a more detailed theoretical description, in analogy to the more prominent region of the 4*d* shape resonance.

ACKNOWLEDGMENTS

The authors would like to thank Professor Sonntag for his hospitality at HASYLAB and his continuing interest in this work. They would also like to thank Professor Bradshaw and W. Braun for their cooperation and help with the HE-TGM at BESSY. This project was supported by the Bundesminister for Forschung und Technologie (BMFT) under Contract No. 05 314 EX B2-1. The measurement of photoions was performed under Proposal No. 86-073 at the Photon Factory at the National Laboratory for High Energy Physics.

[1]M. O. Krause, in *Synchrotron Radiation Research,* edited by H. Winick and S. Doniach (Plenum, New York, 1980), p. 104.
[2]V. Schmidt, Appl. Opt. **19**, 4080 (1980).
[3]B. Crasemann and F. Wuilleumier, in *Atomic Inner-Shell Physics,* edited by B. Crasemann (Plenum, New York, 1985), p. 281.
[4]M. Ya. Amusia, Comments At. Mol. Phys. **8**, 61 (1979).
[5]A. F. Starace, in *Handbuch der Physik,* edited by W. Mehlhorn (Springer-Verlag, Berlin, 1982), Vol. 31.
[6]H. P. Kelly, Phys. Scr. **T17**, 109 (1987).
[7]D. J. Kennedy and S. T. Manson, Phys. Rev. A **5**, 227 (1972).
[8]J. B. West, P. R. Woodruff, K. Codling, and R. G. Houlgate, J. Phys. B **9**, 407 (1976).
[9]L. Torop, J. Morton, and J. B. West, J. Phys. B **9**, 2035 (1976).
[10]M. O. Krause, T. A. Carlson, and P. R. Woodruff, Phys. Rev. A **24**, 1374 (1981).
[11]S. Southworth, U. Becker, C. M. Truesdale, P. H. Kobrin, D. W. Lindle, S. Owaki, and D. A. Shirley, Phys. Rev. A **28**, 261 (1983).
[12]F. Wuilleumier, M. Y. Adam, P. Dhez, N. Sandner, V. Schmidt, and W. Mehlhorn, Phys. Rev. A **16**, 646 (1977).
[13]B. W. Yates, K. H. Tan, L. L. Coatsworth, and G. M. Bancroft, Phys. Rev. A **31**, 1529 (1985).
[14]A. Fahlmann, M. O. Krause, M. A. Carlson, and A. Svensson, Phys. Rev. A **30**, 812 (1984).
[15]D. W. Lindle, T. A. Ferrett, P. A. Heimann, and D. A. Shirley, Phys. Rev. A **37**, 3808 (1988).
[16]U. Becker, H. G. Kerkhoff, M. Kupsch, B. Langer, D. Szostak, and R. Wehlitz, J. Phys. (Paris) Colloq. **48**, C9-497 (1987).
[17]J. W. Cooper, Phys. Rev. Lett. **13**, 762 (1964).
[18]M. Ya. Amusia, V. K. Ivanov, and L. V. Chernysheva, Phys. Lett. **59A**, 191 (1976); M. Ya. Amusia and V. K. Ivanov, *ibid.* **59A**, 194 (1976).
[19]Z. Altun, M. Kutzner, and H. P. Kelly, Phys. Rev. A **37**, 4671 (1988).

[20]E. Dietz, W. Braun, A. M. Bradshaw, and R. L. Johnson, Nucl. Instrum. Methods A **239**, 359 (1985).

[21]R. Bruhn, E. Schmidt, H. Schröder, B. Sonntag, A. Thevenon, G. Passereau, and J. Flamand, Nucl. Instrum. Methods **208**, 771 (1983).

[22]L. O. Werme, T. Bergmark, and K. Siegbahn, Phys. Scr. **6**, 141 (1972).

[23]H. Aksela, S. Aksela, and H. Pulkkinen, Phys. Rev. A **30**, 865 (1984); H. Aksela, S. Aksela, G. M. Bancroft, K. H. Tan, and H. Pulkkinen, *ibid.* **33**, 3867 (1986).

[24]T. A. Carlson and M. O. Krause, Phys. Rev. Lett. **17**, 1079 (1966).

[25]W. Gudat and C. Kunz, in *Synchrotron Radiation,* Vol. 10 of *Topics in Current Physics,* edited by C. Kunz (Springer-Verlag, Berlin, 1979), p. 55; B. L. Henke, J. P. Knauer, and K. Premaratue, J. Appl. Phys. **52**, 1503 (1981); R. H. Day, P. Lee, E. B. Saloman, and D. J. Nagel, Los Alamos National Laboratory Report No. LA-012-79-1360, 1981 (unpublished).

[26]D. W. Lindle, T. A. Ferrett, P. A. Heimann, and D. A. Shirley, Phys. Rev. A **34**, 1131 (1986); G. C. Angel, J. A. R. Samson, and G. Williams, Appl. Opt. **25**, 3312 (1986).

[27]H. Derenbach, R. Malutzki, and V. Schmidt, Nucl. Instrum. Methods **208**, 845 (1983); S. H. Southworth, A. C. Parr, J. E. Hardis, J. L. Dehmer, and D. M. P. Holland, Nucl. Instrum. Methods A **246**, 782 (1986).

[28]M. Krumrey, F. Schäfers, E. Tegeler, J. Barth, M. Krisch, and R. Wolf, Appl. Opt. **27**, 4336 (1988); M. Krumrey, E. Tegeler, R. Thornagel, and G. Ulm, in Proceedings of the 3rd International Conference on Synchrotron Radiation Instrumentation, Tsukuba, 1988 [Rev. Sci. Instrum. (to be published)].

[29]U. Becker, H. G. Kerkhoff, B. Langer, D. Szostak, and R. Wehlitz (unpublished).

[30]J. B. West and J. Morton, At. Data Nucl. Data Tables **22**, 103 (1978), and references therein.

[31]Y. Sato, T. Hayaishi, Y. Itikawa, Y. Itoh, J. Murakami, T. Nagata, T. Sasaki, B. Sonntag, A. Yagishita, and M. Yoshino, J. Phys. B **18**, 225 (1985).

[32]D. M. P. Holland, K. Codling, J. B. West, and G. V. Marr, J. Phys. B **12**, 2465 (1979).

[33]Th. M. El-Sherbini and M. J. Van der Wiel, Physica **62**, 119 (1972).

[34]M. J. Van der Wiel and G. R. Wight, Phys. Lett. **54A**, 83 (1975).

[35]U. Gelius, J. Electron Spectrosc. Relat. Phenom. **5**, 985 (1974); S. Svensson, N. Martennson, E. Basilier, P. Å. Malmquist, U. Gelius, and K. Siegbahn, Phys. Scr. **14**, 141 (1976); S. Svensson, B. Eriksson, N. Martensson, G. Wendin, and U. Gelius, J. Electron Spectrosc. Relat. Phenom. **47**, 327 (1988).

[36]M. Y. Adam, F. J. Wuilleumier, N. Sandner, S. Krummacher, V. Schmidt, and W. Mehlhorn, Jpn. J. Appl. Phys. **17**, 170 (1978).

[37]S. P. Shannon, K. Codling, and J. B. West, J. Phys. B **10**, 825 (1977).

[38]M. Y. Adam, Ph.D. thesis, Université de Paris–Sud, 1978.

[39]U. Becker, T. Prescher, E. Schmidt, B. Sonntag, and H. E. Wetzel, Phys. Rev. A **33**, 3891 (1986).

[40]P. A. Heimann, D. W. Lindle, T. A. Ferrett, S. H. Liu, L. J. Medhurst, M. N. Piancastelli, D. A. Shirley, U. Becker, H. G. Kerkhoff, B. Langer, D. Szostak, and R. Wehlitz, J. Phys. B **20**, 5005 (1986).

[41]U. Becker, D. Szostak, M. Kupsch, H. G. Kerkhoff, B. Langer, and R. Wehlitz, J. Phys. B (to be published).

[42]A. Zangwill and P. Soven, Phys. Rev. Lett. **45**, 204 (1980); see also G. Wendin, in *X-ray and Atomic Inner-shell Physics (University of Oregon, Eugene, Oregon),* Proceedings of the International Conference on X-ray and Atomic Inner-Shell Physics—1982, AIP Conf. Proc. No. 94, edited by B. Crasemann (AIP, New York, 1982), p. 495.

[43]B. Kämmerling, H. Kossmann, and V. Schmidt, J. Phys. B (to be published).

[44]U. Becker, B. Langer, H.-G. Kerkhoff, M. Kupsch, D. Szostak, R. Wehlitz, P. A. Heimann, S. H. Liu, D. Lindle, T. A. Ferrett, and D. A. Shirley, Phys. Rev. Lett. **60**, 1490 (1988).

[45]A. Reimer, J. Schirmer, J. Feldhaus, A. M. Bradshaw, U. Becker, H.-G. Kerkhoff, B. Langer, D. Szostak, R. Wehlitz, and W. Braun, Phys. Rev. Lett. **57**, 1707 (1986).

[46]G. Wendin and M. Ohno, Phys. Scr. **14**, 148 (1976).